Scientific Research Publishing

Advances in Materials Physics and Chemistry, 2023, 13, 151-160
https://www.scirp.org/journal/ampc
ISSN Online: 2162-5328
ISSN Print: 2162-531X

Influence of Defect Density, Band Gap Discontinuity and Electron Mobility on the Performance of Perovskite Solar Cells

Issiaka Sankara, Soumaïla Ouédraogo, Daouda Oubda, Boureima Traoré, Marcel Bawindsom Kébré, Adama Zongo, François Zougmoré

Département de Physique, Laboratoire de Matériaux et Environnement (LA.M. E)-UFR/SEA, Université Joseph Ki-ZERBO, Ouagadougou, Burkina Faso
Email: sankaraissaka1@gmail.com

How to cite this paper: Sankara, I., Ouédraogo, S., Oubda, D., Traoré, B., Kébré, M.B., Zongo, A. and Zougmoré, F. (2023) Influence of Defect Density, Band Gap Discontinuity and Electron Mobility on the Performance of Perovskite Solar Cells. *Advances in Materials Physics and Chemistry*, **13**, 151-160.
https://doi.org/10.4236/ampc.2023.138011

Received: July 16, 2023
Accepted: August 28, 2023
Published: August 31, 2023

Abstract

In this manuscript, we used the SCAPS-1D software to perform numerical simulations on a perovskite solar cell. These simulations were used to study the influence of certain parameters on the electrical behavior of the cell. We have shown in this study that electron mobility is strongly influenced by the thickness of the absorber, since electron velocity is reduced by thickness. The influence of the defect density shows that above 10^{16} cm^{-3} all the electrical parameters are affected by the defects. The band discontinuity at the interface generally plays a crucial role in the charge transport phenomenon. The importance of this study is to enable the development of good quality perovskite solar cells, while taking into account the parameters that limit solar cell performance.

Keywords

Defect Density, Electron Mobility, Band Gap, Perovskite, SCAPS-1D Software

1. Introduction

3D perovskite, with the general formula $CH_3NH_3PbX_3$ (X = I, Br or Cl), was the Star of the Year 2012 thanks to its remarkable entry into the field of photovoltaics. In just a few years, this material has experienced a meteoric rise and has positioned itself in the global efficiency race, with the latest efficiency certified by the NREL (National Renewable Energy Laboratory) at 22% [1]. This record is due to its good charge carrier transport and mobility properties [2], [3] and has a high absorption coefficient in the right range of wavelengths (corresponding to

the solar spectrum). Its chemical exhibility is a major advantage, enabling molecular engineering of its various components [4]. Recently, these halogenated perovskites have also shown great promise as active materials in light-emitting devices such as light-emitting diodes and lasers. However, despite the rapid progress of perovskite-based devices, and in particular the performance of solar cells, the fundamental properties of the material remain relatively unknown and undocumented. Understanding the mechanisms driving this unprecedented success, and correlating the optical and excitonic properties with the morphology and atomic structure of the material are needed to optimize devices. In this manuscript we will discuss how the variation of certain parameters could affect the performance of the device. These include the influence of electron mobility variation, the combined influence of thickness variation and doping, the influence of conduction band discontinuity as a function of interface recombination rate and, finally, the influence of hole density in the absorber on electrical parameters in general.

2. Materials and Methods

2.1. Structure of a Perovskite Solar Cell

A perovskite solar cell takes the form of a set of thin layers (of the order of a hundred nanometers or microns) deposited on a substrate, usually **Figure 1**. Its operating principle is based on the absorption of light by the perovskite material, which generates free charges (an electron-hole pair) that are photogenerated and extracted using selective contacts. The perovskite material is located in the middle of the photovoltaic cell. Visible sunlight reaching the perovskite layer allows electrons in the valence band to reach the conduction band, generating holes. The electron-hole pair (exciton) rapidly separates the free charges, given that the binding energy of perovskite excitons is low (a few tens of meV at room temperature) [5]. Charges are generated using an electron transport layer (ETL) and a hole transport layer (HTL) on either side of the perovskite. These charges are then diffused to be collected at the contact electrodes of the photovoltaic cell (transparent collection electrode and counter-electrode).

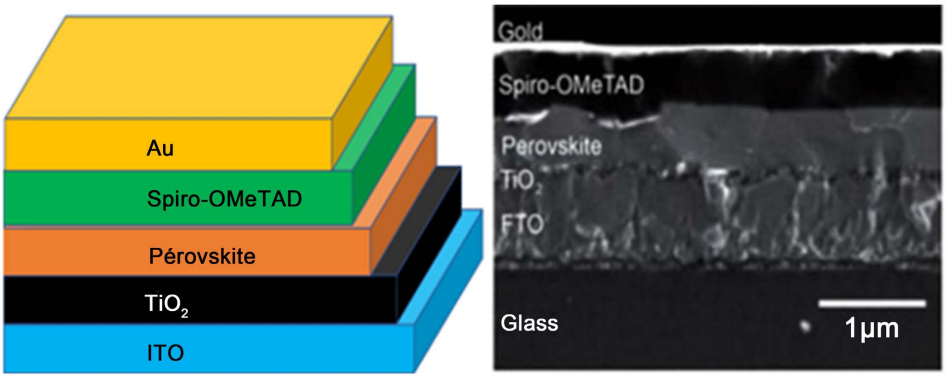

Figure 1. Structure of a perovskite photovoltaic cell and SEM image showing the architecture of a planar heterojunction solar cell based on perovskite materials [4].

2.2. Characterization of the Device

We used one-dimensional SCAPS version.3.2 as the simulation tool. The configuration of the perovskite solar cell structure is as follows: TCO/buffer/interface/perovskite/HTM.

The table below highlights the input parameters for each layer of the TCO, buffer, absorber and HTM are based on TiO_2, $CH_3NH_3PbI_3$-xClx, and (Spiro OMeTAD), respectively. N_A and N_D represent the acceptor and donor densities, ε_r is the relative permeability, χ is the electron affinity, E_g is the band gap energy, μ_n and μ_p are the electron and hole mobilities, and N_t is the defect density. The thicknesses of the TCO, buffer, absorber and HTM were taken from the literature reporting an efficiency of 15.4% [6]. The conductivity types of the TCO, buffer, absorber and HTM are n^+, n, i (or n^-), p^+, respectively, indicating that perovskite solar cells are n-i-p junction typically used in amorphous and microcrystalline silicon-based solar cells. In this study, we assumed $N_t = 2.5 \times 10^{13}$ cm^{-3} in order to obtain electron and hole carrier diffusion lengths (L_n and L_p) at 1 µm, which is a similar value to the experiment [7]. Here, L_n and L_p are identical because all the parameters for the carriers are set identically, which is consistent with the ambipolar characteristics of the carriers [8]. The other input parameters not listed in the table were set in the same way: the effective density of conduction band and valence band states were set at 2.2×10^{18} and 1.8×10^{19} cm^{-3}, respectively. The thermal velocity of the electron and hole was 10^7 cm/s. The energy level of the defect was the center of the band gap and Gaussian distributed with a characteristic energy of 0.1 eV. The defect type was neutral. The electron and hole capture cross-section was 2×10^{-14} cm^2.

Parameters	TCO (SnO_2:F)	Buffer (TiO_2)	IDL1	Absorber (perovskite)	IDL2	HTM
Layer (nm)	500	50	10	330	10	350
N_A (cm^{-3})	-	-	-	-	-	2.10^{18} [7]
N_D (cm^{-3})	2.10^{19}	10^{16}	10^{13}	10^{13}	10^{13}	-
ε_r	9.0	9.0	6.5	6.5 [6]	6.5	3.0 [9]
X (eV)	4.00	3.90 (variable)	3.90 (variable)	3.90 [10]	3.90	2.45 (variable) [11]
E_g (Ev)	3.50	3.20	1.55 (variable)	1.55 [12]	1.55 (variable)	3.00 [11]
N_t (cm^{-3})	10^{15}	10^{15}	10^{17}	$2.5.10^{13}$	10^{17}	10^{15}

SCAPS is used to replicate and study generally thin-film solar cells available at research level, with different buffer layers [13]. From the solution provided by SCAPS, results such as current characteristics in the dark and under illumination can be obtained as a function of temperature. In addition, important information such as electric field distribution, free and trapped carrier concentrations, recombination profiles and individual carrier current densities as a func-

tion of position can be extracted from the SCAPS program. The simulation of the electrical parameters of the cell with SCAPS is based on the numerical solution of three fundamental charge transport equations in semiconductors, which are: Poisson's Equation (1), and the continuity equations for electrons Equation (2) and holes Equation (3)

$$\frac{\mathrm{d}^2\psi(x)}{\mathrm{d}x^2} = \frac{e}{\varepsilon_o\varepsilon_r}\left[p(x) - n(x) + N_D - N_A + \rho_p - \rho_n\right] \tag{1}$$

$$\frac{\mathrm{d}}{\mathrm{d}x}J_n(x) - e\frac{\partial n(x)}{\partial t} - e\frac{\partial \rho_n}{\partial t} = G_n(x) - R_n(x) \tag{2}$$

$$\frac{\mathrm{d}}{\mathrm{d}x}J_p(x) + e\frac{\partial p(x)}{\partial t} + e\frac{\partial \rho_n}{\partial t} = G_p(x) - R_p(x) \tag{3}$$

where ε_0 and ε_r are the vacuum and relative dielectric constants respectively, n and p are the free carrier concentrations of electrons and holes respectively, N_D and N_A are the concentrations of the donor and acceptor, respectively. With ρ_n and ρ_p the charge density of electrons and holes, J_n and J_p are the current density of electrons and holes, R_n and R_p are the electron and hole recombination rates respectively, G_n and G_p are the electron and hole generation rates respectively

3. Results and Discussion

3.1. Electron Mobility as a Function of Absorber Thickness

"An ideal solar cell must be capable of generating highly mobile electrical charges very quickly, so that they don't immediately recombine," explains Jean-Pierre Wolf. These charge carriers also need to live for a long time so that they can be extracted by the electrodes. **Figure 2** shows the influence of electron mobility as a function of absorber thickness. The simulation shows that electrical parameters such as open-circuit voltage V_{CO}, fill factor FF and efficiency all fall with increasing thickness, while current density J_{SC} rises. The thickness of the absorber influences electron mobility. For perovskite solar cells, electron mobility and diffusion length are crucial parameters. As the thickness of the absorber increases, the velocity of the electrons decreases and the parameters fall, because in perovskite solar cells the excitons have a low binding energy, which leads to faster recombination if the electrons are not sufficiently velocity.

3.2. The Influence of Thickness and Doping on Electrical Parameters

Semiconductor doping can be intentional, as in the case of organic photovoltaic solar cells. As demonstrated by Kirchartz *et al.* [14], doping is generally detrimental to the performance of organic solar cells because the electric field may be masked and charges cannot be transported to the electrodes. Doping generally refers to the creation of free charge carriers activated at room temperature, leaving static ions of opposite polarity. **Figure 3** shows the variation in electrical parameters as a function of thickness and doping. This figure shows that all the

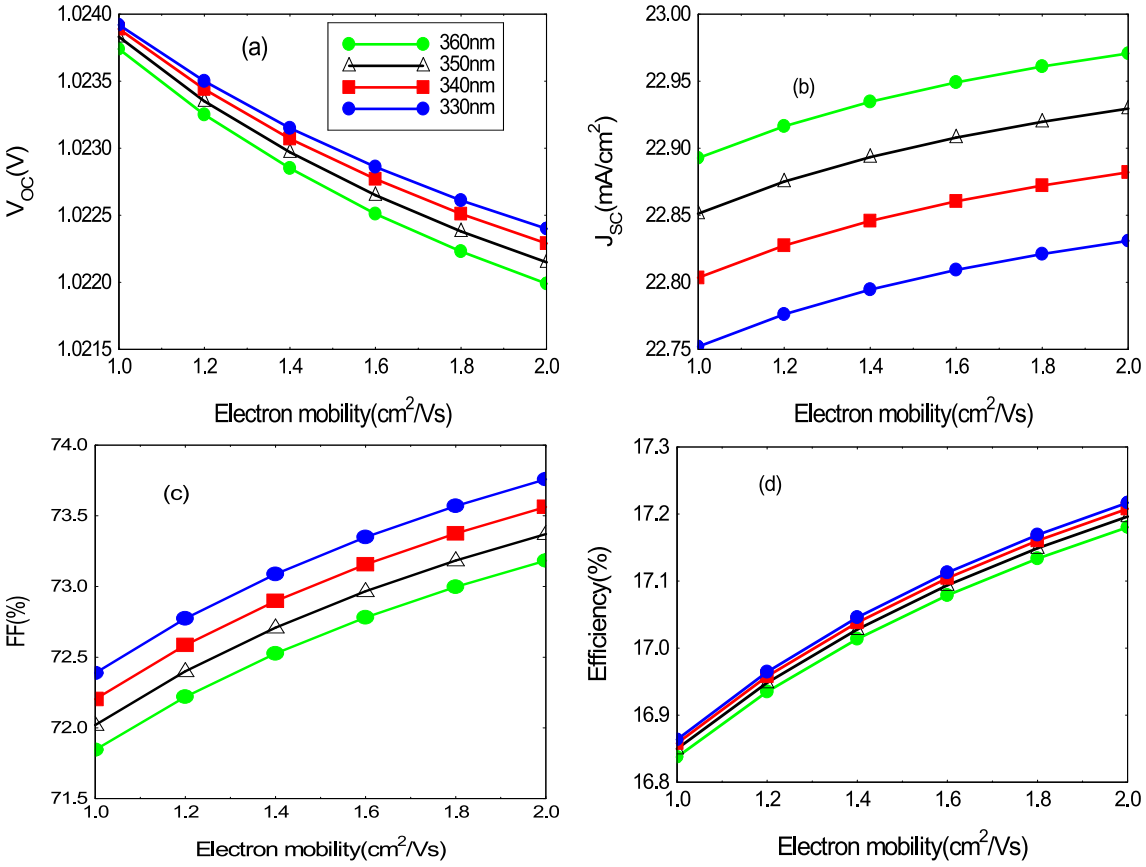

Figure 2. Influence of variation in electron mobility on electrical parameters.

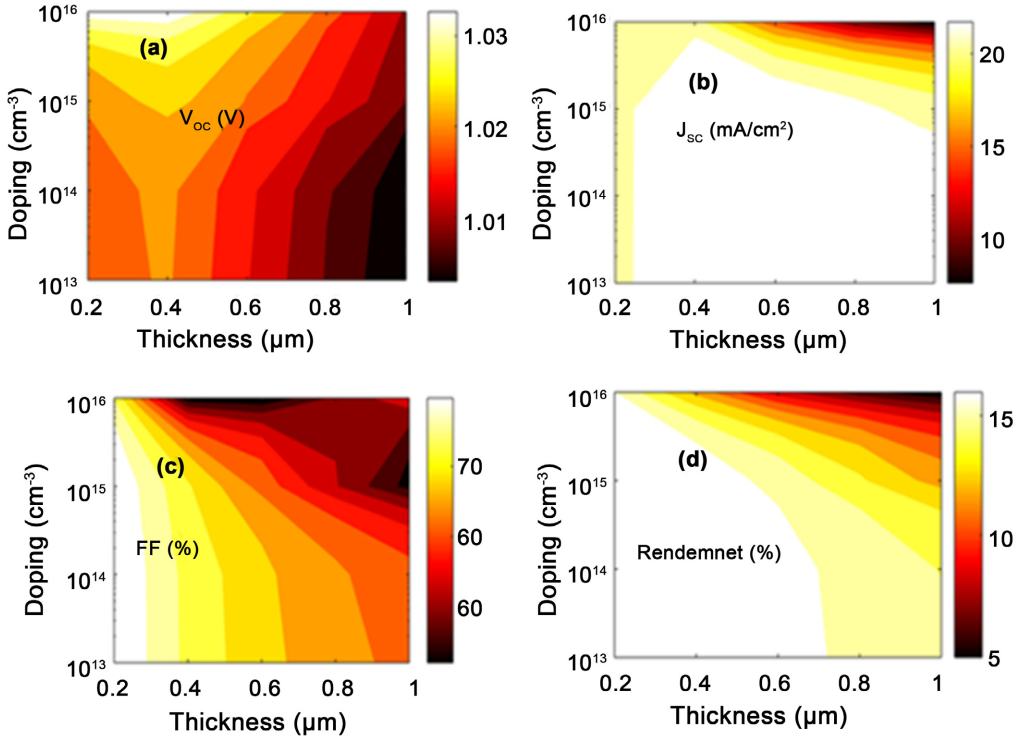

Figure 3. Variation in electrical parameters as a function of thickness and doping.

electrical parameters show better values for a thickness of between 0.2 µm and 0.4 µm for a doping of 10^{16} cm^{-3}. Above 0.4 µm, all the parameters follow the same trend, *i.e.* decrease. As mentioned above by Kirchartz *et al.*, this drop could be due to the fact that charge carriers are not efficiently transported to the electrodes because the electric field that causes charge separation could be masked.

3.3. Conduction Band Offset and Interface Recombination Rate

The most widely used model for studying conduction band offset in a heterojunction solar cell is Anderson's or the electron affinity rule. According to this model, gap deformation between two materials implies the presence of band mismatches in the heterostructures [15]. Discontinuities at the interface generally play a crucial role in the charge transport phenomenon. Minority carriers are confronted with this barrier at the interface, favoring their accumulation and possibly causing recombination. Surface recombinations are calculated using the Shockley-Read-Hall model. The quality of the interface is expressed by the surface recombination rate S. The conduction band offset was calculated by fixing the electronic affinity of the buffer layer, according to the Minemoto model [16]. The equation below shows how this was calculated.

$$\Delta E_C\left(\mathrm{T_iO_2}/\mathrm{perovskite}\right) = \chi_{\mathrm{T_iO_2}} - \chi_{\mathrm{perovskite}} \tag{4}$$

Figure 4 shows that when conduction band offset (ΔE_c) is between [−0.5 - 0 eV]

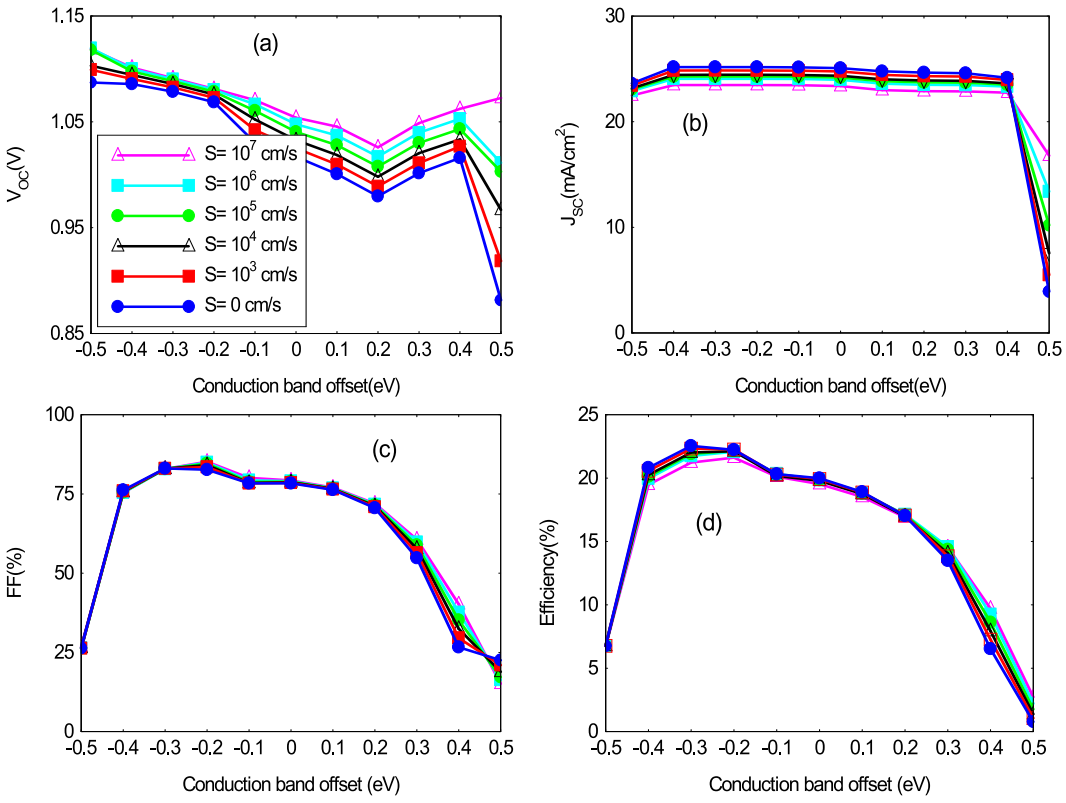

Figure 4. Influence of conduction band offset on electrical parameters as a function of interface recombination rate.

and [0 - 0.5 eV], the fill factor (FF) and efficiency (η) initially increase for the first interval and then both fall for the second interval. There is also a sharp drop in current density (J_{SC}) from a certain value of ΔE_c ($\Delta E_c \geq 0.4$ eV). These variations can be explained by the fact that these discontinuities constitute barriers to the movement of the photogenerated electrons and this necessarily leads to the observed drop in current density (J_{SC}).

Surface recombination is characterized by the variation in the surface recombination rate S. For $\Delta E_c < 0$, the figure shows that V_{CO} depends on the quality of the interface, but is independent of the absorber bandgap and the discontinuity [16] [17]. This result shows that interface defects are the limiting factors for V_{CO} in CIGS devices with a cliff at the interface. For $\Delta E_c > 0.2$ eV, all the electrical parameters are independent of the quality of the interface. Recombination related to peak height become more predominant compared to surface recombination center [18].

3.4. The Influence of the Density of Holes in the Absorber

Impurities in the absorber can increase the density of acceptors in it. The cases most often mentioned are the doping of the absorber with materials such as manganese or nickel in the case of barium titanate ($BaTiO_3$) in order to increase conductivity. The most obvious case is that of doping the absorber with diffusing sodium from the soda glass substrate. Sodium doping of the absorber leads to an increase in the open-circuit voltage (V_{CO}) [15]. In addition, doping must be controlled to optimize the device's performance. These dopants could affect the mobility of the electrons in the conductive layer and therefore the lifetime of the charge carriers. For this reason, it is worth using an oxide such as Al_2O_3 to act as a barrier between the conductive layer and the substrate. **Figure 5** shows the influence of hole density on V_{CO}, J_{SC}, FF and efficiency (η), for different absorber thicknesses. All curves show the same trend for doping between 10^{12} cm^{-3} and 10^{16} cm^{-3} for different thicknesses. For the precise value of 10^{16} cm^{-3}, the open-circuit voltage (V_{CO}) in **Figure 5(a)** shows a peak, while the form factor (FF) in **Figure 5(c)** shows a cliff. Finally, above this value, the open-circuit voltage, current density and efficiency fall sharply, but the form factor increases. The behavior of the open-circuit voltage is explained by its dependence on the width of the space charge zone (ZCEW) and the density of holes in the absorber. An increase in hole density leads to a reduction in the width of the space charge zone and consequently to a variation in V_{CO}, particularly saturation at high values of p. For $w > 330$ nm, the thickness of the absorber should be of the same order of magnitude as the width of the space charge zone [19]. In this case, the effect of absorber doping on the open-circuit voltage remains insignificant. The current density follows the same trend for different absorber thicknesses. It decreases considerably from $p = 10^{16}$ cm^{-3}. However, the decrease in J_{SC} is more abrupt for $w > 330$ nm. For this thickness range, the increase in doping leads to a considerable reduction in the width of the space charge zone, and consequently the

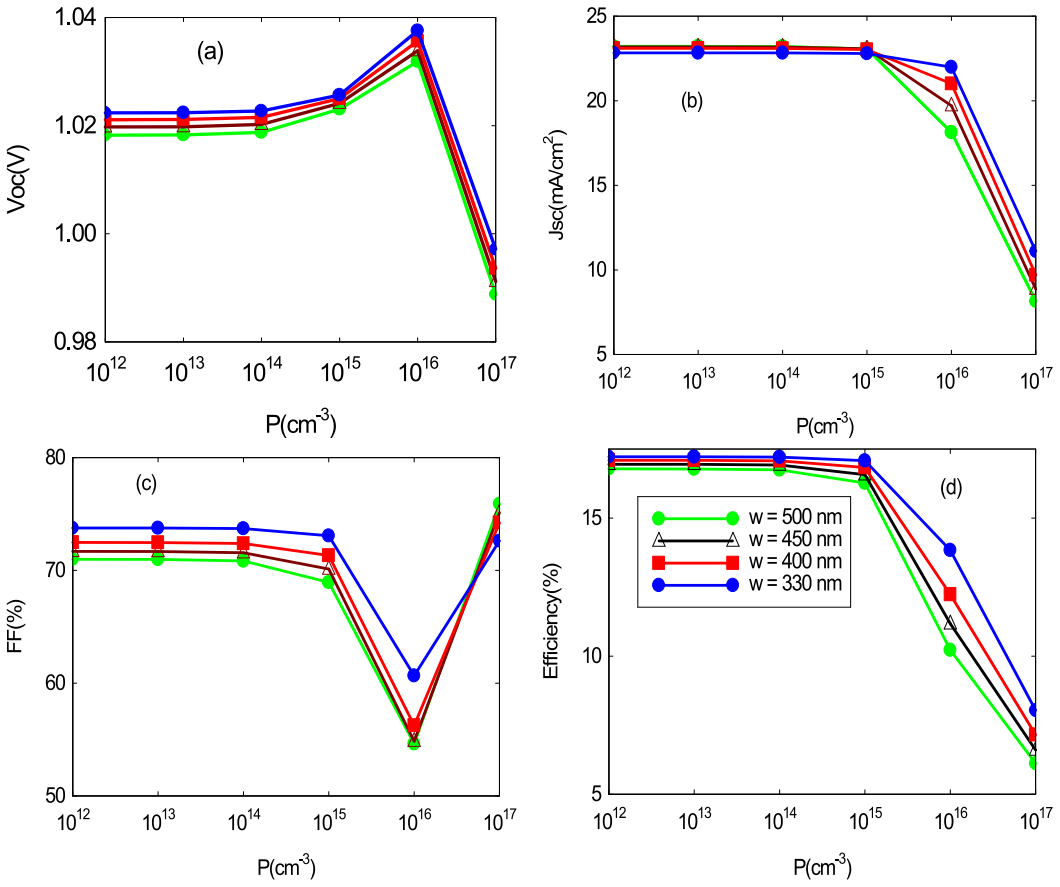

Figure 5. Influence of hole density on: (a) V_{CO}, (b) J_{SC}, (c) FF and η (d) as a function of absorber thickness.

collection of carriers by the junction. The form factor is also affected by the increase in hole density.

4. Conclusion

In this manuscript, we have studied electron mobility, the combined influence of thickness variation and doping, the influence of the conduction band discontinuity as a function of the interface recombination rate and, finally, the influence of the hole density in the absorber on the electrical parameters in general. This study shows that for good open-circuit voltage collection, the interface at the junctions between the buffer layer and the absorber must be of good quality. Also, electron mobility should be faster to avoid recombination of photogenerated carriers and finally, to obtain better electrical parameters, the doping should be of the order of 10^{16} cm^{-3} for a thickness of between 0.2 μm and 0.4 μm.

Conflicts of Interest

The authors declare no conflicts of interest regarding the publication of this paper.

References

[1] (2020) Datalab-53 (2019) Chiffres clés des énergies renouvelables. Edition 2019.

https://www.statistiques.developpement-durable.gouv.fr/sites/default/files/2019-05/datalab-53-chiffres-cles-des-energies-renouvelables-edition-2019-mai2019.pdf

[2] Huang, L., *et al.* (2016) Electron Transport Layer-Free Planar Perovskite Solar Cells: Further Performance Enhancement Perspective from Device Simulation. *Solar Energy Materials and Solar Cells*, **157**, 1038-1047. https://doi.org/10.1016/j.solmat.2016.08.025

[3] Stranks, S.D., *et al.* (2013) Electron-Hole Diffusion Lengths Exceeding 1 Micrometer in an Organometal Trihalide Perovskite Absorber. *Science*, **342**, 341-344. https://doi.org/10.1126/science.1243982

[4] Eperon, G.E., Burlakov, V.M., Docampo, P., Goriely, A. and Snaith, H.J. (2014) Morphological Control for High Performance, Solution-Processed Planar Heterojunction Perovskite Solar Cells. *Advanced Functional Materials*, **24**, 151-157. https://doi.org/10.1002/adfm.201302090

[5] Miyata, A., *et al.* (2015) Direct Measurement of the Exciton Binding Energy and Effective Masses for Charge carriers in an Organic-Inorganic Tri-Halide Perovskite. *Nature Physics*, **11**, 582-587.

[6] Liu, M., Johnston, M.B. and Snaith, H.J. (2013) Efficient Planar Heterojunction Perovskite Solar Cells by Vapour Deposition. *Nature*, **501**, 395-398. https://doi.org/10.1038/nature12509

[7] Stranks, S.D., Eperon, G.E., Grancini, G., Menelaou, C., Alcocer, M.J.P., Leijtens, T., Herz, L.M., Petrozza, A. and Snaith, H.J. (2013) Electron-Hole Diffusion Lengths Exceeding 1 Micrometer in an Organometal Trihalide Perovskite Absorber. *Science*, **342**, 341-344. https://doi.org/10.1126/science.1243982

[8] Ball, J.M., Lee, M.M., Hey, A. and Snaith, H.J. (2013) Low-Temperature Processed Meso-Superstructured to Thin-Film Perovskite Solar Cell. *Energy & Environmental Science*, **6**, 1739-1743. https://doi.org/10.1039/c3ee40810h

[9] Snaith, H.J. and Grätzel, M. (2007) Electron and Hole Transport through Mesoporous TiO_2 Infiltrated with Spiro-MeOTAD. *Advanced Materials*, **19**, 3643-3647. https://doi.org/10.1002/adma.200602085

[10] Hirasawa, M., Ishihara, T., Goto, T., Uchida, K. and Miura, N. (1994) Magnetoabsorption of the Lowest Exciton in Perovskite-Type Compound (CH_3NH_3) PbI_3. *Physica B: Condensed Matter*, **201**, 427-430. https://doi.org/10.1016/0921-4526(94)91130-4

[11] Poplavskyy, D. and Nelson, J. (2003) Nondispersive Hole Transport in Amorphous Films of Methoxy-Spirofluorene-Arylamine Organic Compound. *Journal of Applied Physics*, **93**, 341-346. https://doi.org/10.1063/1.1525866

[12] Noh, J.H., Im, S.H., Heo, J.H., Mandal, T.N. and Seok, S.I. (2013) Chemical Management for Colorful, Efficient, and Stable Inorganic-Organic Hybrid Nanostructured Solar Cells. *Nano Letters*, **13**, 1764-1769. https://doi.org/10.1021/nl400349b

[13] Chelvanathan, P., Hossain, M.I. and Amin, N. (2010) Performance Analysis of Copper-Indium-Gallium-Diselenide (CIGS) Solar Cells with Various Buffer Layers by SCAPS. *Current Applied Physics*, **10**, S387-S391. https://doi.org/10.1016/j.cap.2010.02.018

[14] Neukom, M. (2019) Comprehensive Characterization and Modelling of Operation Mechanisms in Third Generation Solar Cells. https://opus.bibliothek.uni_augsburg.de/opus4/files/63805/characterization_and_modelling_diss_neukom.pdf

[15] Ouédraogo, S., Zougmoré, F. and Ndjaka, J.M.B. (2014) Computational Analysis of the Effect of the Surface Defect Layer (SDL) Properties on Cu (In, Ga) Se_2-Based

Solar Cell Performances. *Journal of Physics and Chemistry of Solids*, **75**, 688-695. https://doi.org/10.1016/j.jpcs.2014.01.010

[16] Minemoto, T., *et al.* (2001) Theoretical Analysis of the Effect of Conduction BAND Offset of Window/CIS Layers on Performance of CIS Solar Cells Using Device Simulation. *Solar Energy Materials and Solar Cells*, **67**, 83-88. https://doi.org/10.1016/S0927-0248(00)00266-X

[17] Minemoto, T. and Murata, M. (2015) Theoretical Analysis on Effect of Band Offsets in Perovskite Solar Cells. *Solar Energy Materials and Solar Cells*, **133**, 8-14. https://doi.org/10.1016/j.solmat.2014.10.036

[18] Sherkar, T.S., *et al.* (2017) Recombination in Perovskite Solar Cells: Significance of Grain Boundaries, Interface Traps, and Defect Ions. *ACS Energy Letters*, **2**, 1214-1222. https://doi.org/10.1021/acsenergylett.7b00236

[19] Gloeckler, M. and Sites, J.R. (2005) Band-Gap Grading in Cu (In, Ga) Se_2 Solar Cells. *Journal of Physics and Chemistry of Solids*, **66**, 1891-1894. https://doi.org/10.1016/j.jpcs.2005.09.087